Steitz, J. A., Wahba, A. J., Laughrea, M., & Moore, P. B. (1977) *Nucleic Acids Res. 4*, 1–15.
Stern, S., Changchien, L.-M., Craven, G. R., & Noller, H. F. (1988a) *J. Mol. Biol. 200*, 291–299.
Stern, S., Moazed, D., & Noller, H. F. (1988b) *Methods Enzymol. 164*, 481–489.
Stern, S., Powers, T., Changchien, L.-M., & Noller, H. F. (1988c) *J. Mol. Biol. 201*, 683–695.
Stern, S., Weiser, B., & Noller, H. F. (1988d) *J. Mol. Biol. 204*, 447–481.
Subramanian, A. R. (1985) *Essays Biochem. 21*, 45–85.
Subramanian, A. R., Rienhardt, P., Kimura, M., & Suryanarayana, T. (1981) *Eur. J. Biochem. 119*, 245–249.
Svensson, P., Changchien, L.-M., Craven, G. R., & Noller, H. F. (1988) *J. Mol. Biol. 200*, 301–308.
Tapprich, W. E., Goss, D. J., & Dahlberg, A. E. (1989) *Proc. Natl. Acad. Sci. U.S.A. 86*, 4927–4931.
Thibault, J., Chestier, A., Vidal, D., & Gros, F. (1972) *Biochimie 54*, 829–835.
Thomas, J. O., & Szer, W. (1982) *Prog. Nucleic Acid Res. Mol. Biol. 27*, 157–187.
Thomas, J. O., Kolb, A., & Szer, W. (1978) *J. Mol. Biol. 123*, 163–176.
Thomas, J. O., Boublik, M., Szer, W., & Subramanian, A. R. (1979) *Eur. J. Biochem. 102*, 309–314.
Vassilenko, S. K., Carbon, P., Ebel, J. P., & Ehresmann, C. (1981) *J. Mol. Biol. 152*, 699–721.
Walleczek, J., Albrecht-Ehrlich, R., Stöffler, G., & Stöffler-Meilicke, M. (1990) *J. Biol. Chem. 265*, 11338–11344.
Wickström, E. (1983) *Nucleic Acids Res. 11*, 2035–2052.
Wickström, E., Heus, H. A., Haasnoot, C. A. G., & van Knippenberg, P. H. (1986) *Biochemistry 25*, 2770–2777.
Wiener, L., Schüler, D., & Brimacombe, R. (1988) *Nucleic Acids Res. 16*, 1233–1250.
Yuan, R. C., Steitz, J. A., Moore, P. B., & Crothers, D. M. (1979) *Nucleic Acids Res. 7*, 2399–2418.

Crystal Structure of the Cytochrome P-450$_{CAM}$ Active Site Mutant Thr252Ala[†,‡]

Reetta Raag,[§] Susan A. Martinis,[∥,⊥] Stephen G. Sligar,[∥] and Thomas L. Poulos*[,§]

Center for Advanced Research in Biotechnology of the Maryland Biotechnology Institute, University of Maryland at Shady Grove, 9600 Gudelsky Drive, Rockville, Maryland 20850, Department of Chemistry and Biochemistry, University of Maryland, College Park, Maryland, and Departments of Biochemistry and Chemistry, University of Illinois, Urbana, Ilinois 61801

Received May 29, 1991; Revised Manuscript Received September 10, 1991

ABSTRACT: The crystal structure of a cytochrome P-450$_{CAM}$ site-directed mutant in which the active site Thr252 has been replaced with an Ala (Thr252Ala) has been refined to an *R* factor of 0.18 at 2.2 Å. According to sequence alignments (Nelson & Strobel, 1989), Thr252 is highly conserved among P-450 enzymes. The crystallographic structure of ferrous camphor- and carbon monoxide-bound P-450$_{CAM}$ (Raag & Poulos, 1989b) suggests that Thr252 is a key active site residue, forming part of the dioxygen-binding site. Mutation of the active site threonine to alanine produces an enzyme in which substrate hydroxylation is uncoupled from electron transfer. Specifically, hydrogen peroxide and "excess" water are produced instead of the product, 5-*exo*-hydroxycamphor. The X-ray structure has revealed that a local distortion in the distal helix between Gly248 and Thr252 becomes even more severe in the Thr252Ala mutant. Furthermore, a solvent molecule not present in the native enzyme is positioned in the dioxygen-binding region of the mutant enzyme active site. In this location, the solvent molecule could sterically interfere with and destabilize dioxygen binding. In addition, the active site solvent molecule is connected, via a network of hydrogen bonds, with an internal solvent channel which links distal helix residues to a buried Glu side chain. Thus, solvent protons appear to be much more accessible to dioxygen in the mutant than in the wild-type enzyme, a factor which may promote hydrogen peroxide and/or water production instead of substrate hydroxylation. On the basis of crystallographic and mutagenesis data, a proton delivery pathway involving residues Lys178/Arg186, Asp251, and Thr252 is proposed for wild-type P-450$_{CAM}$. Coordinates of structures discussed in this paper have been submitted to the Brookhaven Protein Data Bank (Bernstein et al., 1977).

The cytochrome P-450 superfamily of enzymes catalyzes many different types of oxidative reactions involved in endogenous metabolic processes including steroid hormone and bile acid biosynthesis and fatty acid metabolism. These enzymes are also involved in detoxification of foreign compounds and have been implicated in carcinogenic transformation (Nebert et al., 1981; Nebert & Gonzalez, 1987; Anders, 1985). Recent reports indicate that P-450s also may be involved in yeast spore wall formation (Eckerstorfer et al., 1991) and possibly in fungal denitrification pathways (Shoun, 1991). The enormous variety of processes P-450 enzymes are involved in as well as the seemingly limitless number of their potential substrates are well represented by a recent review (Guengerich, 1991). As a result of their broad involvement in biochemical processes, there is much interest in structure–function relationships of P-450s with aims including the design of P-450 inhibitors and the engineering of novel P-450s with specificities

[†] Supported in part by NIH Grant GM 33688 (to T.L.P.) and by NIH Grants GM 31756, GM 33775, and RR 01811 (to S.G.S.).

* Address correspondence to T.L.P. at CARB, 9600 Gudelsky Dr., Rockville, MD 20850. Address as of Jan. 1, 1992: Department of Molecular Biology and Biochemistry, University of California, Irvine, Irvine, CA 92717.

[‡] Coordinates have been deposited in the Brookhaven Protein Data Bank and assigned numbers as follows: 2CP4, camphor-bound Thr252Ala mutant P-450$_{CAM}$ (data set 252A1); 3CP4, 11-week adamantane-bound wild-type P-450$_{CAM}$ (data set ADAM8); 4CP4, recombinant wild-type camphor-bound P-450$_{CAM}$ (data set NCAM4).

[§] University of Maryland.
[∥] University of Illinois.
[⊥] Present address: Department of Biology, Massachusetts Institute of Technology, Cambridge, MA 02139.

0006-2960/91/0430-11420$02.50/0

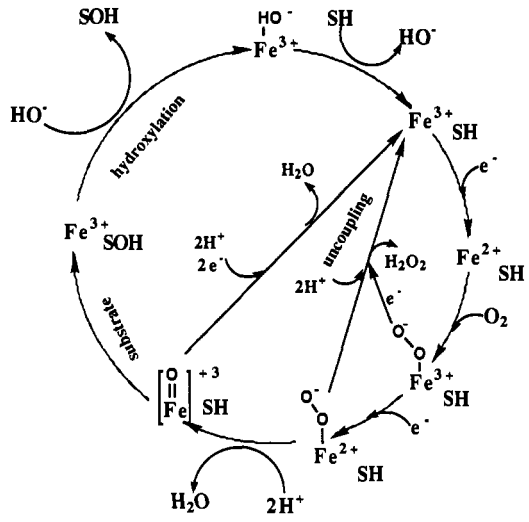

FIGURE 1: P-450 reaction cycle [modified from Atkins and Sligar (1988a)]. SH and SOH represent camphor (substrate) and 5-*exo*-hydroxycamphor (product), respectively. Uncoupling reactions compete with substrate hydroxylation. Efficiency refers to the percentage of reducing equivalents utilized toward substrate oxidation, as opposed to hydrogen peroxide/excess water production.

toward hazardous waste components.

The best characterized P-450 is the bacterial camphor hydroxylase P-450$_{CAM}$ (Gunsalus et al., 1974; Debrunner et al., 1978; Gunsalus & Sligar, 1978; Ullrich, 1979; Wagner & Gunsalus, 1982). This is also the only P-450 enzyme for which crystallographic structures have been determined. These structures include those of the camphor-bound enzyme (Poulos et al., 1985, 1987), the substrate-free enzyme (Poulos et al., 1986), and the ferrous carbon monoxide- and camphor-bound ternary enzyme complex (Raag & Poulos, 1989b). The substrate-free and -bound structures correspond to the first two steps of the reaction cycle of cytochrome P-450$_{CAM}$, shown in Figure 1. The CO–camphor–P-450$_{CAM}$ structure may be used as a model for the ferrous dioxygen- and substrate-bound intermediate. In addition, structures have been determined for P-450$_{CAM}$ complexed with several inhibitors and alternate substrates (Poulos & Howard, 1987; Raag et al., 1990; Raag & Poulos, 1989a, 1991a,b). In combination with biochemical data (White et al., 1984; Fisher & Sligar, 1985; Atkins & Sligar, 1988b, 1989), these structures have provided valuable insight into factors controlling substrate metabolism in P-450s.

The P-450$_{CAM}$ catalytic cycle can be short-circuited in such a way that molecular oxygen is reduced to hydrogen peroxide or two molecules of water, instead of being utilized toward substrate hydroxylation. These compromising side reactions are referred to as uncoupling (Figure 1) and may be promoted by certain substrates as well as by mutations (Atkins & Sligar, 1988b, 1989; Martinis et al., 1989; Imai et al., 1989). On the basis of crystallographic evidence, it has been suggested that disordered active site solvent may lead to substrate-induced uncoupling (Raag & Poulos, 1991a,b). Here we report the structure of the uncoupled Thr252Ala[1] active site mutant of P-450$_{CAM}$ and describe several ways in which this mutation may promote uncoupling and compromise substrate hydroxylation.

Materials and Methods

P-450$_{CAM}$ was purified and crystallized according to procedures that have been described previously (Poulos et al., 1982; Unger et al., 1986; Atkins & Sligar, 1988b). Briefly, 10 μL of ammonium sulfate solution in a buffer of 50 mM potassium phosphate, pH 7.0, 250 mM KCl, and 50 mM dithiothreitol was injected into several 250-μL capillary tubes with precipitant concentrations ranging from 66 to 70% in increments of 2%. Next, 10 μL of the purified substrate-free enzyme at a concentration of about 0.8–1.0 mM was carefully layered over the the ammonium sulfate to form a sharp protein–precipitant interface. Tubes were sealed with Parafilm, and crystals appeared within about three days at temperatures of both 7 and 20 °C. With the Thr252Ala enzyme, we found that lower protein concentrations (0.8 mM) and lower temperatures (7 °C) gave better results than did higher protein concentrations (1 mM) and/or higher temperatures (20 °C). In contrast to wild-type P-450$_{CAM}$, the Thr252Ala mutant usually produced large amounts of needle clusters and precipitate, and single crystals suitable for diffraction analysis were quite rare. This phenomenon is possibly related to our observation of considerably more ordered solvent, much of it near intermolecular contacts, at the surface of the mutant than of the wild-type enzyme (see below).

All crystalline P-450$_{CAM}$ complexes we have studied have essentially identical unit cell dimensions. Wild-type camphor-bound P-450$_{CAM}$ (Poulos et al., 1987) has cell dimensions of 108.7, 103.9, and 36.4 Å. The Thr252Ala mutant reported here (data set 252A1) has dimensions of 108.0, 104.2, and 36.2 Å. As with all other P-450$_{CAM}$ structures we have determined, the ones reported here crystallize in the space group $P2_12_12_1$ with one molecule per asymmetric unit. P-450$_{CAM}$ contains 414 amino acid residues.

In preparation for data collection, crystals were soaked in a mother liquor consisting of 40% saturated ammonium sulfate, 0.05 M potassium phosphate, and 0.25 M KCl at pH 7.0, with saturating amounts of substrate. X-ray diffraction data were collected from single crystals of two different camphor-bound Thr252Ala–P-450$_{CAM}$ complexes using a Siemens area detector/Rigaku rotating anode and were processed and scaled using the XENGEN program package (Howard et al., 1987). The highest resolution data (complete to about 2.2 Å; data set 252A1) were obtained from a crystal soaked for 2 h in camphor-saturated mother liquor; a 4-day soak of another crystal resulted in data complete to about 2.5-Å resolution (data set 252A2). Both independently determined structures were found to be in excellent agreement structurally. To ensure that recombinant P-450$_{CAM}$ is structurally identical to the protein isolated from *Pseudomonas putida* (Poulos et al., 1985, 1987), diffraction data were also collected from several crystals of recombinant wild-type P-450$_{CAM}$ which had been soaked in camphor-saturated mother liquor. The best data were obtained from a crystal soaked for 1 day (data set NCAM4). Data collection statistics are presented in Table I. Also presented are data for recombinant wild-type P-450$_{CAM}$ crystals soaked for 11 weeks in either camphor (NCAM3) or adamantane (ADAM6-7 and ADAM8; the former data set includes data from two crystals scaled together). The adamantane structures were found to be intermediate between the wild-type and Thr252Ala mutant in terms of distal helix structure (see Discussion). With the exception that camphor occupancy appears to have been incomplete following the 11-week soak, the NCAM3 structure is otherwise identical to the original ferric camphor-bound wild-type P-450$_{CAM}$ structure determined by Poulos et al. (1985, 1987).

The somewhat high R_{sym} values (Table I) may reflect the use of recombinant P-450$_{CAM}$ for all structures determined in this study, although no significant structural differences were

[1] Abbreviations: F_c, calculated structure factors; F_o, observed structure factors; R factor, $\sum|F_o - F_c|/\sum F_o$; rms, root mean square; Thr252Ala denotes the mutant generated by replacing the wild-type Thr252 residue by Ala.

Table I: Summary of P-450$_{CAM}$ Data Collection

	data set					
	252A1	252A2	NCAM4	ADAM6-7	ADAM8	NCAM3
resolution	2.1 Å	2.4 Å	2.1 Å	2.1 Å	2.3 Å	2.1 Å
no. observs	106 045	67 326	56 897	45 746	52 078	86 653
R_{sym}[a]	0.086	0.099	0.087	0.067	0.094	0.072
% data to	3.8 Å 100%	4.3 Å 100%	3.8 Å 100%	3.8 Å 100%	4.2 Å 100%	3.8 Å 99%
	3.0 Å 100%	3.4 Å 100%	3.0 Å 100%	3.0 Å 97%	3.4 Å 100%	3.0 Å 97%
	2.6 Å 100%	3.0 Å 100%	2.7 Å 98%	2.7 Å 84%	2.9 Å 98%	2.6 Å 95%
	2.4 Å 100%	2.7 Å 100%	2.4 Å 96%	2.4 Å 73%	2.7 Å 95%	2.4 Å 92%
	2.2 Å 99%	2.5 Å 98%	2.2 Å 89%	2.2 Å 67%	2.5 Å 91%	2.2 Å 86%
	2.1 Å 65%	2.4 Å 60%	2.1 Å 55%	2.1 Å 62%	2.3 Å 48%	2.1 Å 73%
$I/\sigma(I)$	2.4 Å 2.0	2.7 Å 1.8	2.4 Å 1.6	2.7 Å 2.6	3.4 Å 5.1	2.4 Å 6.5
	2.2 Å 1.0	2.5 Å 1.0	2.2 Å 1.0	2.4 Å 1.1	3.0 Å 1.3	2.2 Å 4.2
	2.1 Å 0.5	2.4 Å 0.6	2.1 Å 0.7	2.2 Å 0.6	2.7 Å 0.5	2.1 Å 2.4

[a] $R_{sym} = \sum|Ii - \{Ii\}|/\sum Ii$, where Ii = intensity of the ith observation and $\{Ii\}$ = mean intensity.

Table II: Summary of P-450$_{CAM}$ Crystallographic Refinement

	data set					
	252A1	252A2	NCAM4	ADAM6-7	ADAM8	NCAM3
enzyme	T252A	T252A	Thr252	Thr252	Thr252	Thr252
substrate	camphor	camphor	camphor	adamantane	adamantane	camphor
soak time	2 h	4 days	1 day	11 weeks	11 weeks	11 weeks
resoln (Å)	10.0–2.1	10.0–2.4	10.0–2.1	10.0–2.1	10.0–2.3	10.0–2.1
uniq refls	22 942	15 785	19 351	14 802	15 241	19 960
refls used[a]	16 775	11 601	13 830	9362	6671	17 545
initial R[b]	0.222	0.209	0.200	0.351	0.339	0.220
final R[b]	0.179	0.153	0.164	0.179	0.163	0.192
rms deviation of (in Å)						
bond dists	0.020	0.023	0.024	0.019	0.021	0.022
bond angls	0.034	0.038	0.038	0.035	0.039	0.033
dihedrals	0.034	0.038	0.041	0.039	0.044	0.038

[a] Reflections with $I \geq 2\sigma(I)$; I = intensity. [b] $R = \sum|F_o - F_c|/\sum F_o$ calculated with data for which $I \geq 2\sigma(I)$. Initial R was calculated with wild-type P-450$_{CAM}$ coordinates (Poulos et al., 1987) and camphor included (NCAM3/NCAM4), camphor coordinates not included (ADAM6-7/ADAM8), or camphor included and Ala substituted for Thr252 (252A1/252A2).

observed between the recombinant wild-type enzyme and native P-450$_{CAM}$ purified from *P. putida* (Poulos et al., 1987). Note also that data for the 11-week adamantane-bound wild-type crystals is of considerably lower resolution than for the other complexes (Table I). Statistically significant data extend only to roughly 2.6 and 3.0 Å for data sets ADAM6-7 and ADAM8, respectively. Numerous unsuccessful attempts were made to obtain 11-week adamantane-bound wild-type crystals with better diffraction quality. Failure in this regard may indicate long-term motion in these complexes with catalytic relevance (see Discussion).

Crystallographic refinement was carried out using the restrained parameters–least-squares package of programs (Hendrickson & Konnert, 1980) and is summarized in Table II. Initial $F_o - F_c$ and $2F_o - F_c$ difference Fourier maps were calculated using coordinates based on the wild-type camphor–P-450$_{CAM}$ structure refined to 1.7-Å resolution (Poulos et al., 1987), including all 204 water molecules and diffraction data obtained from the crystalline complexes. $F_o - F_c$ maps were contoured at $\pm 3\sigma$, and $2F_o - F_c$ maps were contoured at +0.5 and $+1\sigma$ (σ is the standard deviation of the electron density map). Fitting of an atomic model to electron density maps was done with the molecular modeling package FRODO (Jones, 1978) operating on an Evans and Sutherland graphics station.

Based on electron density maps as well as subsequent refinement, recombinant wild-type P-450$_{CAM}$ was judged to be identical to the native enzyme which was isolated from *P. putida* (data not shown). Initial Thr252Ala mutant maps were calculated with wild-type coordinates, with and without camphor included to confirm that camphor had bound successfully. Positive substrate electron density as well as negative density around the Thr252 side chain indicated that the crystallized protein had bound camphor and was indeed the mutant enzyme. New maps were then calculated using Ala coordinates in place of Thr at position 252, and with camphor included. Large changes were observed in the distal helix region of the mutant enzyme, with respect to the wild-type structure. Thus, maps were also calculated with distal helix residues 247–255 omitted from the phase calculation. Such "omit" maps were also used later in the refinement process to ensure an unbiased interpretation of the electron density. Significant adjustments had to be made to distal helix residues 250–255 in the mutant enzyme model to obtain an acceptable fit to the electron density.

Initial maps also showed major changes in the internal solvent region "behind" the distal helix, between residues 252 and Glu366. Coordinate shifts resulting from refinement were successful in eliminating most solvent-related difference density in this region. However, positive difference density was also present in the dioxygen-binding groove, indicating that a water molecule was present *in the active site* of the camphor-bound mutant enzyme. Oddly enough, similar positive difference density was found distributed primarily on the surface of the mutant in both structure determinations, indicating that many (25–30) additional solvent molecules not observed in the native structure are bound by the mutant enzyme. With the exception of the 204 solvent molecules present in the wild-type structure, additional water molecules were not included in the mutant model until considerable refinement had convinced us they were not artifactual. Another unusual aspect of both Thr252Ala structures determined was that several residues, again mainly on the protein surface, were found to have side chains occupying two conformations. In general, we have not

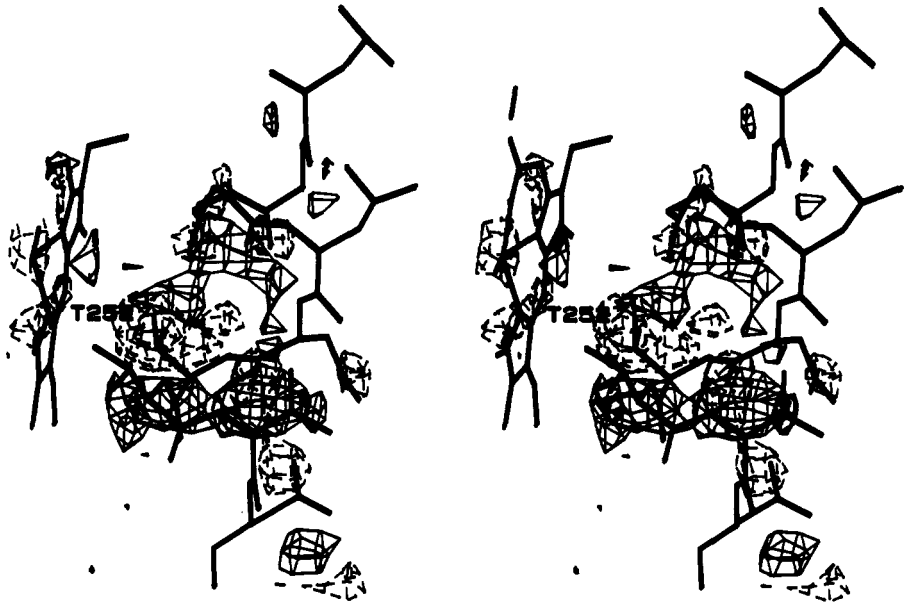

FIGURE 2: Initial $F_o - F_c$ difference electron density map for the Thr252Ala mutant (252A1) of P-450$_{CAM}$, calculated with diffraction amplitudes from the crystalline camphor-bound mutant protein and phases from camphor-bound wild-type P-450$_{CAM}$ coordinates (Poulos et al., 1987). The map is contoured at $\pm 3\sigma$ with negative and positive density depicted as dashed and solid lines, respectively. The wild-type P-450$_{CAM}$ coordinates are shown. A portion of the heme appears on the left side of the figure, and the distal helix is on the right. Note $\pm 3\sigma$ $F_o - F_c$ electron density indicating major conformational rearrangements in distal helix residues, especially Thr252 and Asp251. Negative density around the Thr252 side chain confirms that the mutant contains an alanine at this position. Negative density around the Asp251 carbonyl oxygen, with positive density nearby, indicates that the carbonyl group is in a different position in the mutant enzyme, with respect to the wild-type structure. Electron density corresponding to the solvent molecule bound in the dioxygen-binding groove was not evident in initial maps since the abundant electron density corresponding to movements of nearby distal helix residues and negative density surrounding the model Thr252 side chain was masking it at this stage. Once alanine was substituted for T252 in the model, density corresponding to this water appeared.

observed many double conformations in previous substrate– or inhibitor–P-450$_{CAM}$ structure determinations. The most noteworthy of the residues with two conformations is Thr101, an active site residue. The side chain of Thr101 hydrogen bonds with the Tyr96 side-chain OH group, and Tyr96 also hydrogen bonds with the substrate.

Structures were judged to have refined sufficiently once $F_o - F_c$ maps showed little or no interpretable density when contoured at 3σ. Initial $F_o - F_c$ and final $2F_o - F_c$ maps are shown in Figures 2 and 3. Final maps were also calculated omitting the internal solvent channel (no. 523, 566, and 687) and active site water (no. 720) molecules from the phase calculation, to confirm their presence. Refined models were subjected to additional refinement without bond, angle, or nonbonded contact distance restraints to better estimate active site distances. However, restrained and unrestrained models were virtually identical structurally. Comparison of both coordinate and temperature factor shifts was carried out as described elsewhere (Poulos & Howard, 1987).

Results

On the basis of X-ray diffraction data of about 2.2-Å resolution, recombinant wild-type P-450$_{CAM}$ is structurally identical to native P-450$_{CAM}$ isolated from *P. putida* (Poulos et al., 1987). Therefore, all structural changes observed in the Thr252Ala structure are attributable to the mutation and not to the use of recombinant enzyme. Initial and final electron density maps of the Thr252Ala mutant are shown in Figures 2 and 3, and a comparison of mutant and wild-type coordinates is presented in Figure 4. Several major structural changes are apparent in the Thr252Ala mutant of P-450$_{CAM}$ with respect to the wild-type enzyme. For the most part, these changes are concentrated in the active site region of the distal helix and include the following:

(1) A large movement (1.4 Å) of the side-chain C_β of the mutated residue Ala252 away from the dioxygen-binding groove with respect to the position occupied by the wild-type Thr252 C_β.

(2) The carbonyl group of the preceding residue, Asp251, has flipped by about 120° to point away from Val396 in the active site and toward the distal helix. In the mutant enzyme, the carbonyl oxygen of Asp251 is able to form a characteristic α-helical hydrogen bond with the backbone amide proton of Asn255. Besides these conformational differences in distal helix residues between wild-type and Thr252Ala mutant structures, no other significant structural changes *in protein residues* have been observed.

(3) Major rearrangements have occurred in the solvent channel between residue 252 and the buried Glu366. In the wild-type enzyme, three solvent molecules are enclosed "behind" the distal helix between Thr252 and Glu366, and not directly accessible to the active site. In the mutant enzyme, the internal water nearest the active site has "dropped" by about 2.3 Å to a location nearer to the heme and "below" the distal helix. In its new location this third water (water no. 687) is directly accessible to the active site.

(4) Finally, a fourth solvent molecule is located *in* the active site, in the distal helix groove between residue 252 and Gly248. This location places the new water (water no. 720) in direct contact with camphor.

Replacement of Thr252 with Ala eliminates the Thr252 side-chain–Gly248 peptide oxygen hydrogen bond. However, the rearrangement of solvent structure near the active site compensates by allowing at least one and possibly two new hydrogen bonds with Gly248. In the mutant, waters 687 and 720 are, respectively, 2.5 and 3.2 Å from the Gly248 peptide oxygen atom. In contrast, water 687 is 3.6 Å from the peptide oxygen of Gly248 in the wild-type enzyme.

Electron density corresponding to the fourth water (water no. 720) is well-defined and discrete, probably since it may hydrogen bond with the carbonyl oxygens of residues 247 and 248 as well as with the amide proton of residue 252. This

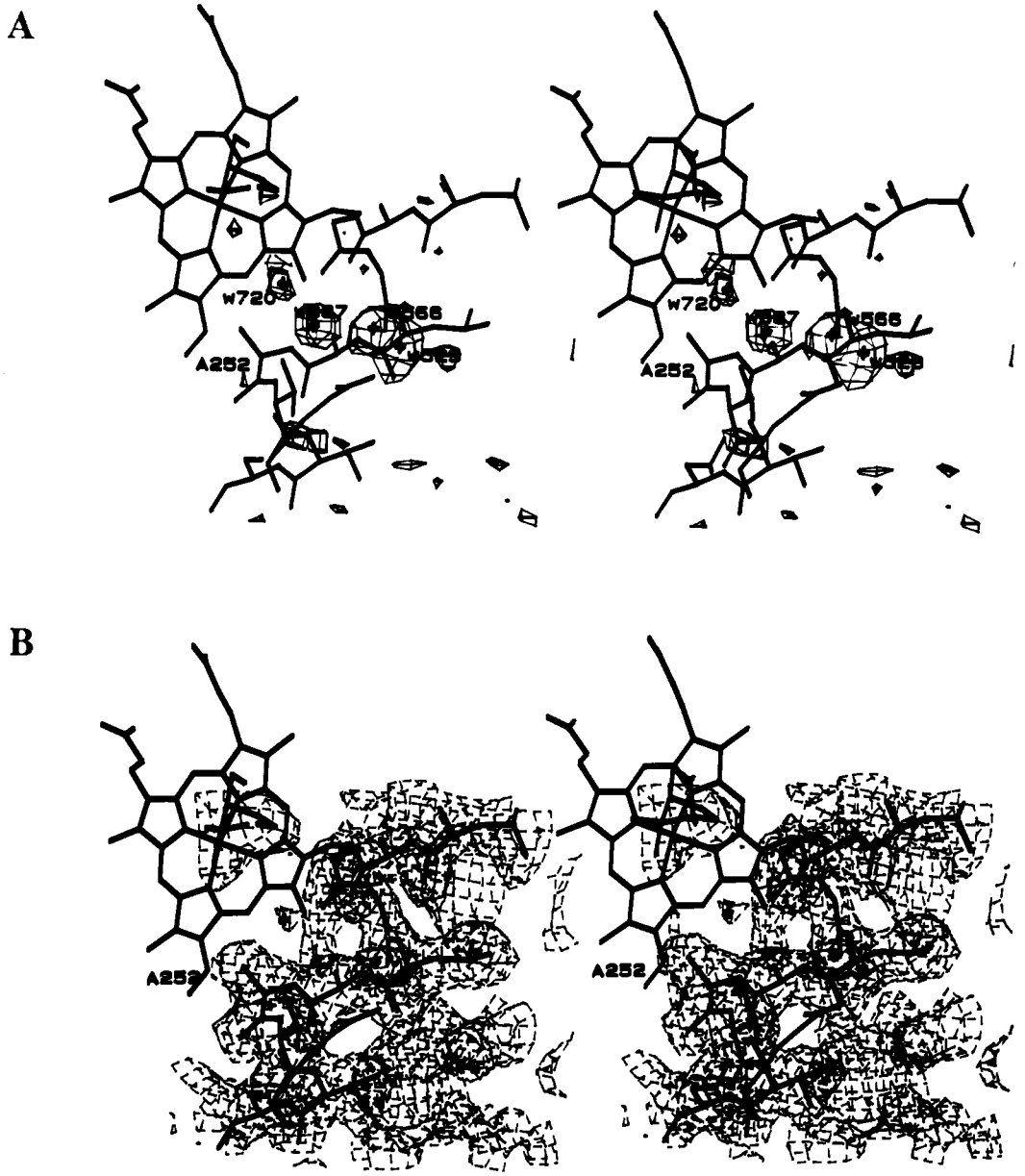

FIGURE 3: Final (A) $F_o - F_c$ and (B) $2F_o - F_c$ electron density maps for the Thr252Ala mutant of P-450$_{CAM}$. Coordinates shown are those of the refined Thr252 Ala mutant. The heme and a portion of camphor are in the upper left part of the figure. The distal helix is on the lower right. Internal solvent channel and active site solvent molecules (four altogether) were omitted from the phase calculation for the maps shown, providing unbiased evidence of their presence. Note electron density corresponding to all four water molecules shown.

situation is in contrast to the disordered solvent we believe may occupy the active site in the presence of substrates that have been found to promote uncoupling of wild-type P-450$_{CAM}$ (Atkins & Sligar, 1987; Raag & Poulos, 1991a,b). The active site water can be accommodated in a very specific location in the mutant enzyme since the movement of the Ala252 side chain and the flip of the Asp251 carbonyl together create a considerably larger distal helix groove than occurs in wild-type P-450$_{CAM}$. In contrast to the three internal solvent channel waters which have occupancies ranging from about 0.77 for the one nearest the distal helix (no. 687) to 1.0 for the two nearer to Glu366 (no. 523 and 566), the fourth active site solvent molecule (no. 720) has an occupancy of only 0.55. The temperature factor of this water, however, is about 18 Å^2, which is only slightly higher than that of camphor.

In general, temperature factors of protein and camphor atoms are very similar in mutant and wild-type P-450$_{CAM}$ structures. Some of the largest differences (only about 5 Å^2 higher in the mutant) are observed in loop regions between elements of secondary structure, in the central portion of the distal helix and in helices C and E which contact the distal helix. The rms temperature factor difference, calculated with all heme and protein atoms, between the Thr252Ala mutant and wild-type P-450$_{CAM}$ is about 2.1–2.5 Å^2 (crystals 252A2 and 252A1, respectively).

All of the P-450$_{CAM}$ structures we have determined have distorted hydrogen bonding in the distal helix, with approximately a four-residue stretch lacking the ideal α-helical n to $n + 4$ carbonyl oxygen to amide proton hydrogen bond. The distortion starts approximately 1 residue earlier in the Thr252Ala mutant than in the wild-type enzyme (n = 247 vs 248) and an ideal hydrogen-bonding pattern also resumes about 1 residue earlier in the mutant (n = 251 vs 252).

In both independently determined Thr252Ala structures, the side chain of Thr101 was found to occupy two conformations, one corresponding to that observed in the wild-type enzyme. We have found no obvious explanation for the occurrence of the second conformation. However, Thr101 is located near the distal helix (in particular Leu244), and enhanced mobility of the distal helix in the mutant enzyme may

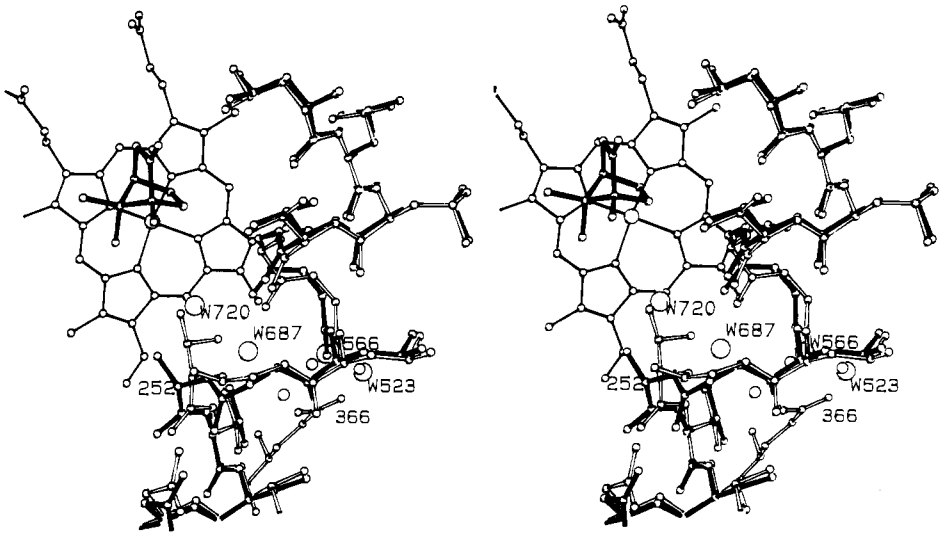

FIGURE 4: Comparison of wild-type (clear bonds) and Thr252Ala mutant (solid bonds) P-450$_{CAM}$ coordinates. Wild-type solvent molecules are depicted as small unlabeled spheres; water molecules of the mutant as large labeled spheres. The internal solvent channel between Thr252 and Glu366 contains three buried solvent molecules (no. 523, 566, and 687) in the wild-type enzyme (Poulos et al., 1987). In contrast, one of the internal waters of the Thr252Ala mutant enzyme (no. 687) has moved toward a location in which it is accessible to the heme and probably dioxygen. Furthermore, the mutant contains an additional solvent molecule (no. 720) in the dioxygen-binding groove in the active site, between Thr252 and Gly248. This structure indicates that solvent may play a key role in uncoupling of electron transfer from substrate hydroxylation in the mutant enzyme. Large structural changes between wild-type and the Thr252Ala mutant of P-450$_{CAM}$ are confined to distal helix residues and solvent surrounding the helix. Thus, the positions of camphor, the heme group, and Glu366 are essentially identical for both structures and are shown here only for the mutant.

simply be propagating to this residue. In both native and new conformations, the side-chain hydroxyl of Thr101 is within hydrogen-bonding distance of Tyr96.

Discussion

Functional Consequences of Thr252 Mutations. On the basis of alignments of known P-450 sequences, several amino acids are highly conserved, notably the residue corresponding to Thr252 in P-450$_{CAM}$ (Nelson & Strobel, 1988, 1989; Gotoh & Fujii-Kuriyama, 1989). In the P-450$_{CAM}$ structure (Poulos et al., 1985, 1987), Thr252 is located in the distal helix, and its side-chain hydroxyl hydrogen bonds with the carbonyl oxygen of Gly248 to form a slightly larger helical groove than would occur in an ideal α-helix (Poulos et al., 1987). On the basis of the ferrous CO–camphor–P-450$_{CAM}$ structure (Raag & Poulos, 1989b), this groove could be the dioxygen-binding site.

Camphor hydroxylation by wild-type P-450$_{CAM}$ occurs with 100% efficiency: all NADH consumed is channeled toward 5-*exo*-hydroxycamphor production. However, when the highly conserved active site Thr252 is replaced with alanine, the efficiency drops to only 5–6% and electrons are channeled to produce hydrogen peroxide and water instead of product (Imai et al., 1989; Martinis et al., 1989). These reactions competing with substrate hydroxylation (Figure 1) are referred to as uncoupling (Staudt et al., 1974; Zhukov & Achakov, 1982; Gorsky et al., 1984; Atkins & Sligar, 1987, 1988a). Similar losses in catalytic activity toward substrates have been observed upon mutation of the corresponding conserved threonine in eukaryotic P-450s (Furuya et al., 1989a,b; Imai & Nakamura, 1989).

The crystal structure suggests that the cause for uncoupling is the greater access of solvent to the active site in the mutant enzyme. Dioxygen–heme complexes are unstable in protic solvents, undergoing rapid autooxidation presumably due to protonation of oxygen (Brinigar et al., 1974). Hence, the ready availability of solvent protons to the oxygen binding site in the Thr252Ala mutant destabilizes the oxy complex, resulting in uncoupling.

Adamantane-Induced Conformational Changes in the Distal Helix. Before considering the role(s) of Thr252, it is of value to describe substrate-induced structural changes we have observed in and around the distal helix, as a result of unintentionally soaking wild-type crystals for an extended period of time in adamantane (data not previously published). It is important to note that these structural changes occurred in the *wild-type* enzyme. Internal water 687, the solvent molecule located nearest to the distal helix, forms hydrogen bonds with several distal helix residues (Gly249, Thr252, Val253, Val254) as well as with another internal solvent molecule (no. 566). However, water 687 is not present in all wild-type substrate–P-450$_{CAM}$ complexes we have investigated. Notably, this water molecule appears to be missing when the enzyme is soaked for a few days with certain compounds known [camphane (Atkins & Sligar, 1988b)] and suspected (adamantane) to induce uncoupling (Raag & Poulos, 1991a). Moreover, when wild-type P-450$_{CAM}$ was soaked inadvertently for 11 weeks in adamantane (henceforth referred to as "aged" adamantane structures), not only was water 687 absent, but dramatic structural differences were observed in distal helix residues, especially in Asp251 and Thr252. In fact, the distal helix of the "aged" adamantane structures appears to be structurally intermediate between the distal helices of wild-type and Thr252Ala mutant P-450$_{CAM}$.

In both "aged" adamantane structures, the carbonyl group of Asp251 is about half-way through its "flip" from the wild-type to the Thr252Ala position. Furthermore, the C_β atom of Thr252 has moved approximately 1.1 Å away from the dioxygen-binding groove in the "aged" adamantane structures and 1.4 Å in the Thr252Ala mutant, with respect to the camphor-bound wild-type enzyme. Despite this large movement, Thr252 in the "aged" adamantane structures retains the Thr252 side chain to Gly248 peptide carbonyl oxygen hydrogen bond, although the distance has increased from 2.5 Å (wild-type, camphor-bound) to about 3.0 Å. In contrast, wild-type P-450$_{CAM}$ soaked ("aged") for 11 weeks in camphor was identical to the original wild-type camphor-bound structure determined by Poulos et al. (1987; data not shown). Thus all

Table III: Distal Helix Dihedral Angles

	data set						
	NCAM3	NCAM4	ADAM6-7	ADAM8	252A1	252A2	ideal
Gly 248							
ϕ	−63	−63	−68	−64	−66	−64	−64
ψ	−41	−52	−34	−34	−47	−53	−40
Gly249							
ϕ	−68	−64	−60	−59	−69	−66	−64
ψ	−45	−47	−62	−67	−42	−51	−40
Leu250							
ϕ	−80	−79	−83	−77	−85	−72	−64
ψ	−38	−36	−18	−18	−27	−26	−40
Asp251							
ϕ	−106	−103	−111	−109	−99	−107	−64
ψ	0	3	−35	−42	−55	−58	−40
residue 252							
ϕ	−103	−109	−82	−71	−69	−73	−64
ψ	−66	−71	−61	−60	−45	−40	−40
Val253							
ϕ	−61	−57	−52	−56	−66	−60	−64
ψ	−36	−33	−38	−40	−43	−39	−40
Val254							
ϕ	−52	−52	−52	−54	−52	−57	−64
ψ	−54	−53	−58	−59	−58	−64	−40
Asn255							
ϕ	−70	−70	−67	−64	−65	−61	−64
ψ	−42	−39	−39	−43	−42	−39	−40

three internal solvent channel water molecules are present in the "aged" *camphor*-bound wild-type structure.

Not only are there two instead of three internal solvent channel waters present in the "aged" adamantane wild-type structures, but there also is no active site water present (even at 0.25σ), with the exception of the distal axial heme ligand found with short soak times (Raag & Poulos, 1991a). This finding suggests that the distal helix groove is able to expand in conjunction with major structural changes in residues 251–252, *without the presence of a crystallographically ordered solvent molecule in the groove to induce such changes.* Furthermore, since water 687 has moved by over 2 Å toward the heme in the Thr252Ala mutant enzyme, mutual stabilization may be occurring between water 687 in its internal location and the Thr252 side chain in the camphor-bound wild-type enzyme. Although absence of water 687 from the "aged" adamantane structures may destabilize the side chain of Thr252, facilitating its movement away from Gly248, it is not obvious why the internal water should be missing. It may be that high adamantane mobility (25–30 Å^2) is causing the observed Thr252 side-chain movement and only secondarily destabilizing water 687.

In any case, the "aged" adamantane structures suggest that the internal solvent channel may have a structural role in maintaining the dioxygen-binding groove at the presumably optimal size observed in wild-type camphor-bound P-450$_{CAM}$. In fact, it appears that water 687 helps to stabilize the distal helix in a somewhat unfavorable conformation (especially considering residues 251 and 252). In both Thr252Ala (mutant) and "aged" adamantane (wild-type) structures, backbone ϕ and ψ angles for residues 251 and 252 are significantly closer (by 20°–40°) to ideal values than they are in the wild-type camphor-bound structure (Table III). Thus, the internal solvent channel may function in a manner similar to the cation ligated to the carbonyl oxygen of Tyr96 (Poulos et al., 1987): as structural stabilization for an energetically strained protein conformation which is presumably critical to successful catalysis.

In light of the "aged" adamantane structures, it is possible that Thr252 side-chain motion may also account for some of the residual active site density observed in the presence of norcamphor, camphane, and adamantane following short soaks and which had been interpreted as disordered solvent (Raag & Poulos, 1991a). These highly mobile substrates appear to be revealing a dynamic potential of the distal helix which is not seen when camphor binds.

Role of Thr252. Imai et al. (1989) have suggested that Thr252 might operate as an acid catalyst by donating a proton to oxygen during substrate hydroxylation. However, when Thr252 is replaced by Asn, about 57% of O_2 consumed is utilized toward camphor hydroxylation (Shimada et al., 1990). Since both Thr252 and Asn252 are productive enzymes, it seems unlikely that Thr252 donates its hydroxyl proton to dioxygen. The p*K*'s of both threonine and asparagine side chains are probably much too high for either to become unprotonated during the catalytic cycle. On the other hand, both Thr and Asn have hydrophilic side chains and could accept external protons to operate in a proton shuttle without becoming negatively ionized. Another possibility is that the hydrogen bond between the Thr252 side chain and the Gly248 carbonyl oxygen is the critical factor in preventing uncoupling. Asn could conceivably also form such an interaction with Gly248. This scenario is also supported by the Thr252Ser mutant which hydroxylates camphor with 85% efficiency and presumably contains a similar 252 side chain to distal helix backbone hydrogen bond (Imai et al., 1989; Imai & Nakamura, 1989).

As Thr252 is one of the only hydrophilic residues in the P-450$_{CAM}$ active site, another potential role of this residue is to hydrogen bond with, and hence stabilize, bound dioxygen. Hydrogen bonding between O_2 and Thr252 would require a disruption of the hydrogen-bonding pattern observed in the native enzyme and considerable side-chain rotation and perhaps movement of Thr252. Nevertheless, considering the range of motion we have observed in the distal helix of the wild-type enzyme, such active site rearrangement in the presence of O_2 is a distinct possibility.

Besides Thr252, other residues near the active site are conserved. As can be seen from Figure 4, an internal channel consisting of three well-defined solvent molecules connects the highly conserved Thr252 residue with the side chain of a buried glutamate residue (Glu366) in wild-type camphor-bound

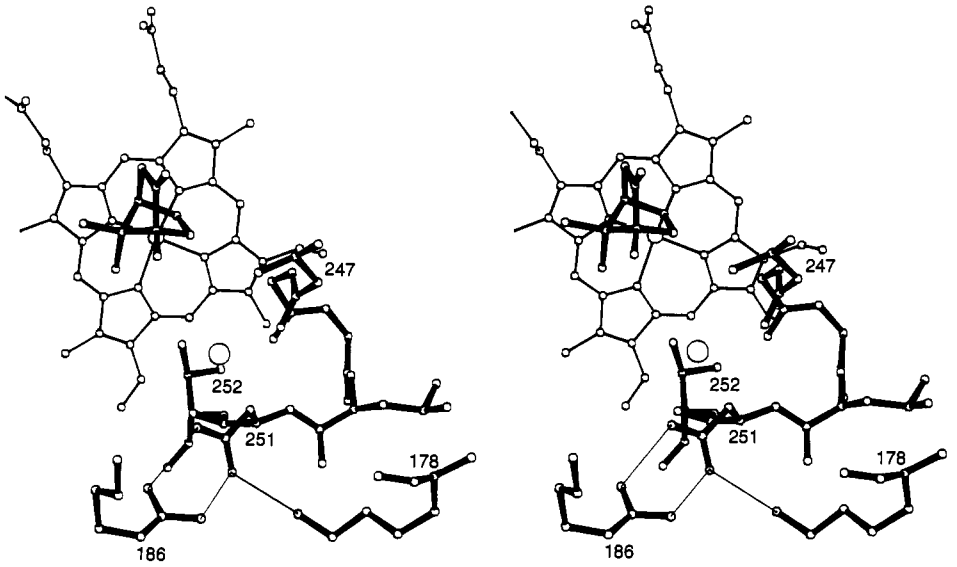

FIGURE 5: Approximate location of energetically favorable water-binding site identified by Wade (1990). The water is depicted as a large sphere between Thr252, Asp251, and Val247. This water is considerably farther from the distal helix dioxygen-binding groove than is the active site water (no. 720) found in the Thr252Ala structure (Figure 4) and would not be expected to be nearly as accessible to iron-bound oxygen. A water in this location may function in shuttling protons between Lys178/Arg186, Asp251, Val247, Thr252, and iron-bound oxygen during the catalytic cycle in P-450$_{CAM}$. Ion pairs between Lys178, Asp251, and Arg186 are indicated as thin lines.

P-450$_{CAM}$. Glu366 is found in 42 of 53 aligned P-450 sequences (Nelson & Strobel, 1989) and is part of the proximal helix (helix L), which is one of the most highly conserved segments in all P-450s. Conservation of the two residues capping the ends of the internal solvent channel suggests that other P-450s may share this structural feature.

Protons are required both for substrate hydroxylation as well as for the dioxygen dissociation as hydrogen peroxide and/or dioxygen cleavage and reduction to water which are observed in uncoupled P-450s (Figure 1; Atkins & Sligar, 1987). We have suggested that the internal solvent channel between Thr252 and Glu366 may provide the protons required during the P-450 catalytic cycle (Raag & Poulos, 1991a,b) although another possible proton-donating network is discussed below. In wild-type P-450$_{CAM}$, the solvent channel behind the distal helix is not accessible to the active site, according to calculated van der Waals surfaces of surrounding residues. However, the side-chain hydroxyl of Thr252 is close enough (3.5 Å) to the nearest solvent channel water molecule (no. 687) that a weak hydrogen-bonding interaction may be present. The Thr252 side chain also is indirectly hydrogen bonded with the internal water channel via the Gly248 carbonyl oxygen and the amide proton of Val253. The fact that the internal solvent channel in wild-type P-450$_{CAM}$ is separated from the active site by a hydrogen-bonding network involving several distal helix residues suggests that, if the solvent channel provides protons for catalysis, proton delivery to the activated oxygen is probably under fine control by the enzyme.

In the Thr252Ala mutant there also exists a hydrogen-bonded network which links distal helix residues, four water molecules, and Glu366. However, in contrast to the native enzyme, two of these solvent molecules are directly accessible to the active site in the mutant. One solvent molecule occupies the dioxygen-binding pocket between residues 248 and 252 (Figure 4), strongly suggesting that direct contact between solvent and dioxygen is at least partially responsible for uncoupling electron transfer from substrate hydroxylation. Solvent in contact with dioxygen could favor hydrogen peroxide and/or water production in at least two ways: (1) it may physically interfere with and thus destabilize dioxygen binding and (2) it may allow protons to be delivered to dioxygen in an uncontrolled manner, bypassing mechanisms which may be regulating proton delivery in the wild-type enzyme.

An Alternative Source of Protons. In contrast to the Thr252Ala mutant which shows little decrease in O_2 consumption rate with respect to the wild-type enzyme, mutation of Lys178, Arg186, or especially of Asp251 to Ala results in a dramatic decrease in O_2 consumption: 65%, 36%, and 0.2% of the wild-type rate, respectively (Shimada et al., 1990). Asp251 is located in the distal helix, adjacent to Thr252, and an acidic residue is highly conserved at this position (Nelson & Strobel, 1989). The side chain of Asp251 forms salt bridges with Lys178 and Arg186, both of which are located in a solvent-filled crevice at the surface of P-450$_{CAM}$. A positively charged residue is also conserved at the Lys178 position (Nelson & Strobel, 1989). Although one function of these ion pairs may be to stabilize global protein structure, these bridges may also form part of a proton delivery path in wild-type P-450$_{CAM}$, mediating proton transfer from surface water to the active site (see Figure 5).

Recent theoretical work pertains to proton delivery in P-450$_{CAM}$. Wade (1990) has identified an energetically favorable water-binding site in the wild-type P-450$_{CAM}$ active site which is well-defined by surrounding van der Waals surfaces (Figure 5). A solvent molecule positioned in this site would be within hydrogen-bonding distance of both the carbonyl oxygen of Val247 and the side-chain OD1 of Asp251. It is interesting that a water molecule in this location has been observed crystallographically in only one P-450$_{CAM}$ structure, that of the enzyme complexed with the inhibitor 2-phenylimidazole (Poulos & Howard, 1987). This fact together with the observation that there is a hydrogen bond between the inhibitor and water molecule suggest that solvent bound in this location may be somewhat unstable. Furthermore, since changes in Asp251 and Thr252 in the presence of 2-phenylimidazole resemble those observed in the Thr252Ala mutant structure, water binding in this location may be contingent upon such distal helix rearrangements. Since it binds to heme groups at a greater angle than carbon monoxide does, dioxygen itself may initiate distal helical changes which result in the binding of a solvent molecule, completing a potential proton delivery path.

Modeling suggests that a solvent molecule in the location identified by Wade (1990) could move slightly and rotate within its cavity to hydrogen bond with either (1) the Asp251 side chain and Val247 carbonyl oxygen or (2) the carbonyl oxygens of both Asp251 and Val247. Thus, a solvent molecule originally hydrogen bonded to the Val247 carbonyl oxygen and Asp251 side chain may be induced to reorient in the cavity by an incoming proton from the Asp251 side chain. The new orientation would enable the solvent molecule to donate hydrogen bonds to the carbonyl oxygens of Asp251 and Val247.

A critical feature of this proton delivery model is that the Thr252 side chain should be capable of rotation, which would result in the breaking of its hydrogen-bond to the carbonyl oxygen of Gly248. Such rotation could conceivably reposition the Thr252 side-chain hydroxyl group near the crystallographically observed side-chain methyl group position of Thr252. In this Thr252 orientation, the potential solvent site identified by Wade (1990) would be within hydrogen-bonding distance of not only the carbonyl oxygens of Val247 and Asp251 but also the Thr side-chain hydroxyl group. Thus, a solvent proton could be donated to the side-chain hydroxyl group of Thr252 and ultimately transferred from it to iron-bound dioxygen.

In support of Thr252, not as a proton donor per se but as a link in a proton shuttle, is the flexibility possible in the Thr side chain hydroxyl to dioxygen distance, assuming Thr side-chain rotation. On the basis of simple model building and assuming the Fe–O–O angle of bound dioxygen is roughly 130–135°, the Thr side chain OH to terminal oxygen atom distance could vary in the 3–4-Å range as a function of Thr252 side-chain rotation. Such distance flexibility could allow mutual adjustment in the relative positions of dioxygen and Thr252 and may allow Thr252 to deliver a proton not only to dioxygen but also to a single iron-linked oxygen atom later in the catalytic cycle. This latter short-lived intermediate species should be at a significantly greater distance from the Thr side chain than the terminal atom of iron-bound dioxygen.

The proton delivery model described above is highly dependent on the ability of the Thr252 side chain to rotate. In support of the model, we note that Thr252 side-chain rotation would also clarify other mutagenesis data. When Thr252 is changed to Ser, approximately 15% of O_2 consumed is recovered as H_2O_2 (Imai et al., 1989; Shimada et al., 1990). On the basis of the proton shuttle theory described above, the Thr252 side-chain hydroxyl group rotates to accept a proton and then transfers it to dioxygen. Concurrently, the side-chain methyl group may transiently fill the groove between Thr252 and Gly248. A similar rotation of a Ser252 side chain would leave a more vacant distal helical groove, perhaps allowing the putative water described by Wade (1990) to enter, providing an unregulated source of protons as observed in the Thr252Ala mutant. This scenario could account for the small amount of H_2O_2 observed with the Thr252Ser mutant. It also may account for the fact that 51 out of 53 aligned P-450 sequences contain threonine at the "invariant" 252 location of P-450$_{CAM}$ (Nelson & Strobel, 1989).

The "aged" adamantane structures may help to explain results with the Thr252Val mutant, which generates product with only 24% of consumed O_2, while producing considerably less H_2O_2 (45–51% of O_2 consumed) than other position 252 mutants (Imai et al., 1989; Shimada et al., 1990). The absence of a hydrophilic side chain at position 252 should result in less interaction (mutual stabilization) between the 252 side chain and the internal solvent channel. As observed in the "aged" adamantane structures, the Thr252Val mutant may have its 252 side chain in a position more similar to that of the Thr252Ala mutant than of the wild-type enzyme. However, the bulky valine side chain, as in the "aged" adamantane structures, could inhibit the binding of a solvent molecule in an expanded distal helix groove, unlike the situation in the Thr252Ala mutant.

Furthermore, if Thr252 is the final link in a proton relay network, valine at position 252 would be expected to prevent or slow the operation of such a shuttle. Without solvent in the dioxygen-binding groove, and without a critical proton-transferring side chain, dioxygen may not readily dissociate as H_2O_2. The observation that O_2 consumption in the Thr252Val mutant is about 20–30% that of the wild-type enzyme (Imai et al., 1989; Shimada et al., 1990) is consistent with stabilization of the dioxygen-bound enzyme due to a dearth of protons. It is also in accord with the prediction that water will not be able to bind in the dioxygen-binding groove of the Thr252Val mutant.

Summary

On the basis of the available data, we conclude that the highly conserved active site residue Thr252 in cytochrome P-450$_{CAM}$ has at least two roles and is so highly conserved because every feature of the side chain has a part to play. Structurally, Thr252 interacts with both Gly248 and with water 687 in the internal solvent channel. The solvent channel apparently stabilizes the distal helix in a somewhat distorted conformation which may be critical to limiting the size of the dioxygen-binding groove, preventing solvent from binding there. The crystal structure of the Thr252Ala mutant enzyme strongly suggests that solvent is responsible for the observed uncoupling of enzyme turnover from camphor hydroxylation in this mutant. Uncoupling is probably due to both steric interference between solvent and dioxygen as well as to uncontrolled access of dioxygen to solvent protons, promoting H_2O_2 production.

Together, mutagenesis (Imai et al., 1989; Martinis et al., 1989; Shimada et al., 1990) and crystallographic results (Raag & Poulos, 1991a,b) on cytochrome P-450$_{CAM}$ suggest that solvent must not gain direct access to O_2 if efficient substrate metabolism is to occur. Solvent in contact with dioxygen may supply protons in an uncontrolled manner, promoting H_2O_2 and/or H_2O production, rather than hydroxylated substrate. In contrast, the wild-type enzyme apparently delivers protons to dioxygen in a highly controlled fashion. There now appear to be at least two plausible sources of protons. One is the internal solvent channel linking residues Thr252 and Glu366. A second possibility is that the proton delivery network includes side chains of Lys178 and/or Arg186, Asp251, the carbonyl oxygens of Val247 and Asp251, a solvent molecule which enters the protein following dioxygen binding, and the side chain of Thr252. In this model, the side chain of Thr252 must rotate to accept a proton from Asp251. The methyl group of the threonine side chain may block solvent from entering between Thr252 and Gly248 while Thr252 transfers a proton to O_2.

Acknowledgments

R.R. thanks Walt Stevens and Djordje Filipovic for illuminating comments and Marc Whitlow for use of the X-ray data collection equipment at Genex Corporation.

References

Anders, M. W., Ed. (1985) *Bioactivation of Foreign Compounds*, Academic Press, Inc., New York.

Atkins, W. M., & Sligar, S. G. (1987) *J. Am. Chem. Soc. 109*, 3754–3760.
Atkins, W. M., & Sligar, S. G. (1988a) *Biochemistry 27*, 1610–1616.
Atkins, W. M., & Sligar, S. G. (1988b) *J. Biol. Chem. 263*, 18842–18849.
Atkins, W. M., & Sligar, S. G. (1989) *J. Am. Chem. Soc. 111*, 2715–2717.
Bernstein, F. C., Koetzle, T. F., Williams, G. J. B., Meyer, E. F., Jr., Brice, M. D., Rogers, J. R., Kennard, O., Shimanouchi, T., & Tasumi, M. (1977) *J. Mol. Biol. 112*, 535–542.
Brinigar, W. S., Chang, C. K., Geibel, J., & Traylor, T. G. (1974) *J. Am. Chem. Soc. 96*, 5597–5599.
Debrunner, P. G., Gunsalus, I. C., Sligar, S. G., & Wagner, G. C. (1978) in *Metals in Biological Systems* (Sigel, H., Ed.) Vol. 7, pp 241–275, Marcel Dekker, New York.
Eckerstorfer, M., Briza, P., Koller, H. T., & Breitenbach, M. (1991) in *International Symposium on Cytochromes P-450 of Microorganisms*, July 24–27, pp 34–35, Berlin, Germany.
Fisher, M. T., & Sligar, S. G. (1985) *J. Am. Chem. Soc. 107*, 5018–5019.
Furuya, H., Shimizu, T., Hirano, K., Hatano, M., Fujii-Kuriyama, Y., Raag, R., & Poulos, T. L. (1989a) *Biochemistry 28*, 6848–6857.
Furuya, H., Shimizu, T., Hatano, M., & Fujii-Kuriyama, Y. (1989b) *Biochem. Biophys. Res. Commun. 160*, 669–676.
Gorsky, L. D., Koop, D. R., & Coon, M. J. (1984) *J. Biol. Chem. 259*, 6812–6817.
Gotoh, O., & Fujii-Kuriyama, Y. (1989) in *Frontiers in Biotransformation* (Ruckpaul, K., & Rein, H., Eds.) Vol. 1, pp 195–243, Akademie-Verlag, Berlin.
Guengerich, F. P. (1991) *J. Biol. Chem. 266*, 10019–10022.
Gunsalus, I. C., & Sligar, S. G. (1978) *Adv. Enzymol. Relat. Areas Mol. Biol. 47*, 1–44.
Gunsalus, I. C., Meeks, J. R., Lipscomb, J. D., Debrunner, P. G., & Münck, E. (1974) in *Molecular Mechanisms of Oxygen Activation* (Hayaishi, O., Ed.) pp 559–613, Academic Press, New York.
Hendrickson, W. A., & Konnert, J. H. (1980) in *Computing in Crystallography* (Diamond, R., Ramaseshan, S., & Venkatesan, K., Eds.) pp 1301–1323, Indian Institute of Science, Bangalore.
Howard, A. J., Gilliland, G. L., Finzel, B. C., Poulos, T. L., Ohlendorf, D. H., & Salemme, F. R. (1987) *J. Appl. Crystallogr. 20*, 386–387.
Imai, Y., & Nakamura, M. (1989) *Biochem. Biophys. Res. Commun. 158*, 717–722.
Imai, Y., Shimada, H., Watanabe, Y., Matsushima-Hibiya, Y., Makino, R., Koga, H., Horiuchi, T., & Ishimura, Y. (1989) *Proc. Natl. Acad. Sci. U.S.A. 86*, 7823–7827.
Jones, T. A. (1978) *J. Appl. Crystallogr. 11*, 268–272.
Martinis, S. A., Atkins, W. M., Stayton, P. S., & Sligar, S. G. (1989) *J. Am. Chem. Soc. 111*, 9252–9253.
Nebert, D. W., & Gonzalez, F. J. (1987) *Annu. Rev. Biochem. 56*, 945–993.
Nebert, D. W., Eisen, H. J., Negishi, M., Lang, M. A., Hjelmeland, L. M., & Okey, A. B. (1981) *Annu. Rev. Pharmacol. Toxicol. 21*, 431–462.
Nelson, D. R., & Strobel, H. W. (1988) *J. Biol. Chem. 263*, 6038–6050.
Nelson, D. R., & Strobel, H. W. (1989) *Biochemistry 28*, 656–660.
Poulos, T. L., & Howard, A. J. (1987) *Biochemistry 26*, 8165–8174.
Poulos, T. L., Perez, M., & Wagner, G. C. (1982) *J. Biol. Chem. 257*, 10427–10429.
Poulos, T. L., Finzel, B. C., Gunsalus, I. C., Wagner, G. C., & Kraut, J. (1985) *J. Biol. Chem. 260*, 16122–16130.
Poulos, T. L., Finzel, B. C., & Howard, A. J. (1986) *Biochemistry 25*, 5314–5322.
Poulos, T. L., Finzel, B. C., & Howard, A. J. (1987) *J. Mol. Biol. 195*, 687–700.
Raag, R., & Poulos, T. L. (1989a) *Biochemistry 28*, 917–922.
Raag, R., & Poulos, T. L. (1989b) *Biochemistry 28*, 7586–7592.
Raag, R., & Poulos, T. L. (1991a) *Biochemistry 30*, 2674–2684.
Raag, R., & Poulos, T. L. (1991b) in *Frontiers in Biotransformation* (Ruckpaul, K., Ed.) Vol. 8, Akademie-Verlag, Berlin.
Raag, R., Swanson, B. A., Poulos, T. L., & Ortiz de Montellano, P. R. (1990) *Biochemistry 29*, 8119–8126.
Shimada, H., Makino, R., Imai, M., Horiuchi, T., & Ishimura, Y. (1990) in *Yamada Conference XXVII: International Symposium on Oxygenases and Oxygen Activation*, Dec 10–12, pp 107–110, Kyoto, Japan.
Shoun, H. (1991) in *International Symposium on Cytochromes P-450 of Microorganisms*, July 24–27, pp 100–101, Berlin, Germany.
Staudt, H., Lichtenberger, F., & Ullrich, V. (1974) *Eur. J. Biochem. 46*, 99–106.
Ullrich, V. (1979) *Top. Curr. Chem. 83*, 67–104.
Unger, B. P., Gunsalus, I. C., & Sligar, S. G. (1986) *J. Biol. Chem. 261*, 1158–1163.
Wade, R. C. (1990) *J. Comput. Aided Mol. Des. 4*, 199–204.
Wagner, G. C., & Gunsalus, I. C. (1982) in *The Biological Chemistry of Iron* (Dunford, H. B., Dolphin, D., Raymond, K., & Sieker, L., Eds.) pp 405–412, Riedel, Boston.
White, R. E., McCarthy, M.-B., Egeberg, K. D., & Sligar, S. G. (1984) *Arch. Biochem. Biophys. 228*, 493–502.
Zhukov, A. A., & Archakov, A. I. (1982) *Biochem. Biophys. Res. Commun. 109*, 813–818.